ELSEVIER

Bioelectrochemistry 57 (2002) 155–166

Bioelectrochemistry

www.elsevier.com/locate/bioelechem

Photoelectric response of purple membrane fragments adsorbed on a lipid monolayer supported by mercury and characterization of the resulting interphase

Andrea Dolfi, Giovanni Aloisi, Rolando Guidelli *

Department of Chemistry, Polo Scientifico, University of Florence, Via della Lastruccia 3, 50019 Sesto Fiorentino, Florence, Italy

Received 7 March 2002; received in revised form 31 May 2002; accepted 3 June 2002

Abstract

Purple membrane (PM) fragments were adsorbed on a dioleoylphosphatidylcholine (DOPC) monolayer supported by mercury to investigate the kinetics of light-driven proton transport by bacteriorhodopsin (bR). PM fragments were also adsorbed on a mercury-supported triethyleneoxythiol (TET) monolayer. On both monolayers, the light-on current exhibits a finite, potential dependent stationary component that decreases linearly with a positive shift in the applied potential. The light-on and light-off capacitive photocurrents were interpreted on the basis of a simple equivalent circuit, which accounts for the potential dependence of the stationary light-on current. The potential of zero stationary current is about equal to +0.010 V vs. saturated calomel electrode (SCE) on DOPC-coated mercury. The absolute potential difference across the PM fragments adsorbed at this applied potential was estimated on the basis of extrathermodynamic considerations and amounts to about +260 mV; it compares favorably with the value, +250 mV, of the transmembrane potential of zero stationary current across an oocyte plasma membrane incorporating bR [Biophys. J. 74 (1998) 403.]. The effect of the proton pumping activity of photoexcited PM fragments on the electroreduction kinetics of ubiquinone-10 incorporated in the DOPC monolayer underlying the PM fragments was investigated.
© 2002 Elsevier Science B.V. All rights reserved.

Keywords: Bacteriorhodopsin; Lipid monolayers; Mercury; Proton transport; Transmembrane potential

1. Introduction

Bacteriorhodopsin (bR) is a proton pump present in the purple membrane (PM) isolated from *Halobacterium salinarium*, which pumps protons from the intracellular side of the membrane, where the electrochemical potential of protons is lower, to the extracellular side, where it is higher. The energy required to pump protons is provided by light, which converts the chromophore *all-trans* retinal, attached to the amino group of a lysine residue as a protonated Shiff base, into the *13-cis* isomer. This isomerization brings the proton of the Shiff base close to the carboxyl group of an aspartate residue, starting a cyclic sequence of conformational transitions and protonation–deprotonation steps, which cause the translocation of a proton from the intracellular to the extracellular side. An exhaustive description of the structure of bR and of the molecular mechanism of its function can be found in the literature [1–9].

PM fragments are readily adsorbed on thiol/lipid mixed bilayers supported by gold [10] or by mercury [11,12], as well as on phospholipid monolayers supported by mercury [13], with the extracellular side turned preferentially towards the metal. If the PM fragments adsorbed on a mixed bilayer or a lipid monolayer are illuminated with green light, protons flow from the solution towards the metal side of the PM. This flux must be compensated for by a flux of electrons to the metal surface along the external circuit, to keep the applied potential E constant. This results in a negative capacitive light-on current. Interrupting illumination causes a smaller positive capacitive light-off current.

In the present work, PM fragments were adsorbed on a phospholipid monolayer self-assembled on mercury. This lipid film, whose polar heads are directed towards the solution, has a high mechanical stability, a high resistance to electric fields and a notable reproducibility [14–16]. Over

* Corresponding author. Tel.: +39-055-457-3097; fax: +39-055-457-3098.

E-mail address: guidelli@unifi.it (R. Guidelli).

1567-5394/02/$ - see front matter © 2002 Elsevier Science B.V. All rights reserved.
PII: S1567-5394(02)00117-2

the potential range from −0.2 to −0.75 V/SCE, it behaves like a half-membrane. Thus, it is impermeable to inorganic ions and its differential capacitance is twice that of a black lipid membrane. The capacitive photocurrents were interpreted on the basis of an equivalent circuit that accounts for the potential dependence of the stationary light-on current. Fitting the equivalent circuit to the photocurrents allowed an electrical characterization of the (lipid monolayer)/PM system. The absolute potential difference across the adsorbed PM fragments at the potential of zero stationary light-on current was estimated on the basis of extrathermodynamic arguments. These arguments were also extended to a further system consisting of PM fragments adsorbed on a triethyleneoxythiol (TET) monolayer covalently anchored to the mercury surface. The effect of the local pH change produced by the pumping activity of bR in the cleft between the PM and the phospholipid monolayer upon the kinetics of a lipophilic redox couple incorporated in the latter monolayer was investigated.

2. Experimental section

The water used was obtained from light mineral water by distilling it once, and by then distilling the resulting water from alkaline permanganate. Inorganic salts were purchased from Merck. Merck reagent grade KCl was baked at 500 °C before use to remove any organic impurities. Octadecylamine from Fluka as well as dioleoylphosphatidylcholine (DOPC) from Lipid Products (South Nutfield, Surrey, England) were used as received. PM fragments prepared by the standard protocol [17] were kindly provided by the Max-Planck-Institut für Biophysik, Frankfurt/Main, Germany. Triethyleneoxythiol was kindly provided by the Centre for Self-Organising Molecular Systems, University of Leeds, UK. Monolayers of DOPC were self-assembled on mercury as described earlier [14–16]. The self-assembly of TET on mercury was carried out by keeping a hanging mercury drop electrode (HMDE) immersed in a 4×10^{-2} M solution of the thiol in ethanol for half an hour. The drop was then kept in air for 3 min to allow ethanol to evaporate.

The experimental set-up used in the present measurements is shown in Fig. 1. The whole set-up was contained in the water-jacketed box D, thermostated at 25 °C ± 0.1. The electrolytic solutions in the two cells, A and C, were deaerated by purging with high purity argon for no less than 20 min. The homemade HMDE employed in the measurements is described elsewhere [15,16,18–20]. It was housed in a water-jacketed sleeve on the top of the box, so as to permit the mercury reservoir to be effectively thermostated. A Faraday cage F was used to avoid electrical noise. The vertical movements of the HMDE through the argon/solution interface were realized by means of an oleodynamic system; this ensured the complete absence of

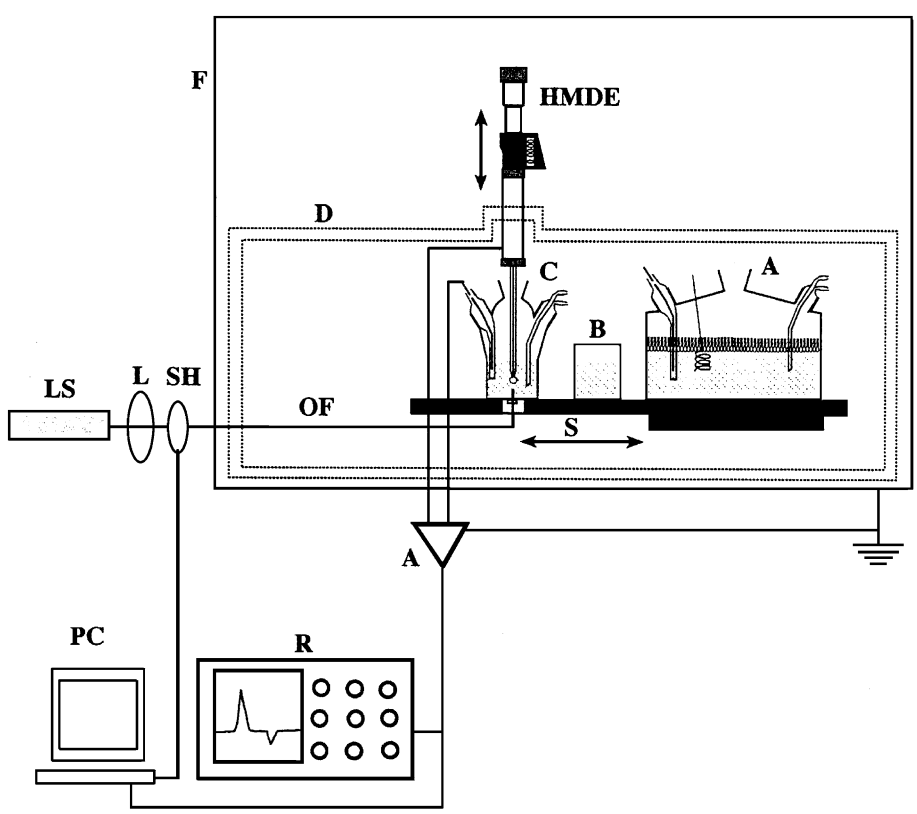

Fig. 1. Experimental set-up. F: Faraday cage; D: water-jacketed box; S: movable support; HMDE: hanging mercury drop electrode; A: three-electrode electrolysis cell; C: two-electrode cell; B: vessel; LS: light source; L: optical fiber coupler; SH: shutter; OF: optical fiber; A: current amplifier; R: recorder.

vibrations while permitting an appreciable range of velocities. A second oleodynamic system was used for the horizontal movements of the movable support S, on which the two cells, A and C, and vessel B were placed; this permitted the HMDE to be positioned above, and then lowered into, any of these three vessels.

The glass cell A was used for monolayer formation and characterization: it contained a platinum counter-electrode, a reference saturated calomel electrode (SCE) and, when required, the working HMDE. With this cell, all measurements were carried out in aqueous 0.1 M KCl. The differential capacitance *C* of the working electrode was measured in cell A by AC voltammetry with a Metrohm Polarecord E506 (Herisau, Switzerland), and was directly obtained from the quadrature component of the AC current. The AC signal had a 10-mV amplitude and a 75-Hz frequency. The system was calibrated with a precision capacitor. Vessel B contained an aqueous dispersion of PM fragments; it was used to adsorb these fragments on DOPC-coated or TET-coated mercury drop electrodes by immersing the electrode in this dispersion for about 10 min. The plexiglass cell C contained an Ag/AgCl (1 M KCl) reference electrode and, when required, the HMDE; it was provided with a quartz optical fiber OF, 0.6 mm in diameter, whose tip was positioned on the cell bottom and was pointed vertically towards the HMDE for its illumination [20]. To attain a good alignment of the optical fiber with the mercury drop, the cell was fixed on an *x*–*y* slide. A syringe connected to a lateral outlet of cell C via silicon tubing (not shown in the figure) allowed electrolytic solutions to be removed from, or injected into, cell C. A small cell containing a composite pH electrode was inserted in line between the syringe and the cell, inside the thermostated box, for an accurate control of pH after the addition of buffered solution. Before each experiment, the stock suspension of PM fragments was sonicated for 1 min to destroy aggregates. The monochromatic light source LS (Helium-Neon Laser, 543.5 nm, Uniphase, model 1675) was focused and collimated using an optical fiber coupler L (Newport, model F-915T) with a maximum output power of ≅ 1.45 mW at the exit of the optical fiber. Incidentally, the absorbance peak of bR has a half-height width of about 100 nm and a maximum at 568 nm [21]. Light pulses were produced using the electromechanical shutter SH (blade shutter and digital shutter controller, Model 845, Newport), which was controlled by the computer PC through a digital-to-analog converter (IOtech DAC488/2). With the above set-up, the maximum light intensity on the mercury drop was attained after about 220 μs. The current generated by illuminating the PM fragments adsorbed on the coated mercury drop under potentiostatic conditions was amplified (Current Amplifier, Keithley 428), filtered (usually 1-kHz low-pass filter), recorded (16-bit analog–digital converter, IOtech ADC488/85A), visualized (Oscilloscope, Tektronix TDS 340A) and stored (Power PC G3, Macintosh). Operation of the experimental set-up and data acquisition were carried out under computer control (GPIB interface, National Instruments board) using a homemade acquisition program written in LabView environment. To increase the signal-to-noise ratio, current vs. time curves were stored upon averaging no less than 15 current transients. The signal was usually sampled at 100-μs intervals over a 3-s time window. The surface area of the mercury drop was of 1.41×10^{-2} cm^2. All potentials are referred to the SCE unless otherwise stated.

3. Results

Before adsorbing the PM fragments on a DOPC-coated HMDE, the good quality of the DOPC monolayer was checked by measuring its differential capacitance in cell A. A compact DOPC monolayer should have a differential capacitance *C* of 1.75–1.80 μF cm^{-2} over a potential range from −0.30 to −0.65 V [14–16], as shown by curve a in Fig. 2. After adsorbing PM fragments in vessel B, the HMDE was transferred to cell C, whose solution did not contain PM, and the differential capacitance was measured again. Adsorption of PM fragments causes an increase in *C* other than over the intermediate potential range from −0.350 to −0.550 V, were *C* remains practically unaltered (see curve b in Fig. 2). This behavior indicates that the PM fragments tend to disorganize the DOPC monolayer by penetrating into the hydrocarbon tail region and/or by tilting the hydrocarbon tails with a resulting decrease in monolayer thickness. Such a behavior is different from that observed by adsorbing PM fragments on mixed hexadecanethiol/DOPC bilayers [11], where the differential capacitance decreases upon PM adsorption throughout the whole potential range investigated. The capacitance remained stable for several hours, just as the bR photoresponse, thus confirming the stability of PM adsorption on the DOPC monolayer even in the absence of PM fragments in the bathing solution.

Illuminating DOPC-coated mercury in the absence of PM fragments produced no electrical signal, thus excluding possible photoartefacts. The initial photoelectrical measure-

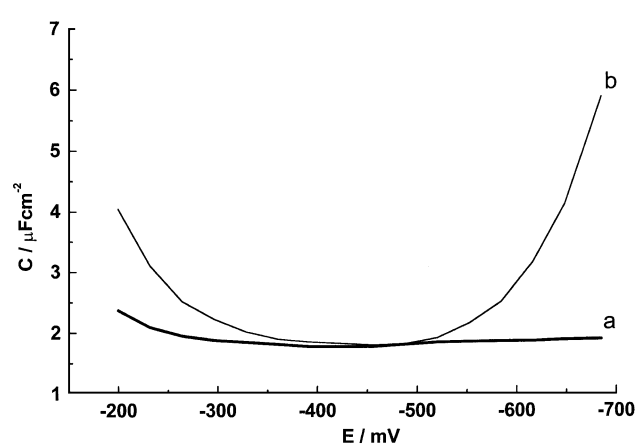

Fig. 2. Plots of the differential capacity *C* of a mercury-supported DOPC monolayer in 0.1 M KCl against the applied potential *E*, both in the absence (a) and in presence (b) of adsorbed PM fragments.

ments with adsorbed PM fragments were carried out with DOPC monolayers incorporating 4 mol% octadecylamine, which is commonly considered to favor the adsorptivity of PM fragments on BLMs as well as their preferential orientation with the extracellular side turned towards the BLM [22,23]. Subsequently, however, it was observed that octadecylamine has no appreciable effect on the sidedness and extent of PM adsorption on mercury-supported DOPC monolayers, nor on the bR photoresponse. Hence, in what follows, no mention will be made to the possible presence of octadecylamine in the DOPC monolayer.

Fig. 3 shows the light-on and light-off currents obtained from PM fragments adsorbed on DOPC-coated mercury at three different applied potentials. The sign of the light-on current is negative, indicating that illumination causes the PM fragments to pump protons from the aqueous solution towards the DOPC monolayer. As in the case of BLMs [23–25], the adsorbed PM fragments are preferentially oriented with the extracellular side towards the monolayer. The translocation of protons across the PM fragments tends to generate a potential difference across them. Under potentiostatic conditions [22,26,27], an equal and opposite potential difference across the whole interphase must, therefore, build up. In other words, a flow of electrons from the reference electrode to the HMDE along the external circuit is required to compensate for the positive charge that is accumulating on the metal side of the PM fragments. This flow of negative charge constitutes the capacitive current detected in the present measurements. Conversely, the light-off current is positive, namely corresponds to a flow of electrons in the opposite direction. This is induced by the movement of the protons, accumulated on the metal side of the PM fragments during illumination, towards the aqueous solution. The light-on current has a stationary component that depends upon the applied potential E, as

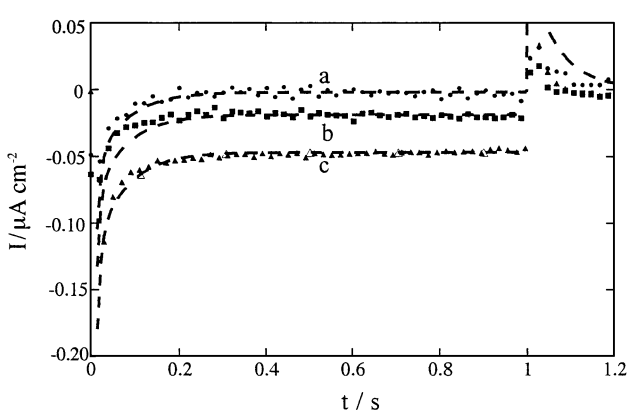

Fig. 3. Negative light-on currents and corresponding positive light-off currents obtained from PM fragments adsorbed on a DOPC-coated mercury electrode immersed in a pH 6.75 buffered solution of 0.1 M KCl + 1 mM KH_2PO_4 + 1 mM K_2HPO_4. Applied potential: 0.00 (a), −0.100 (b) and −0.250 V/SCE (c). Markers are experimental values and the dashed curves are the best fits to the equivalent circuit of Fig. 7. For the parameters employed, see the text.

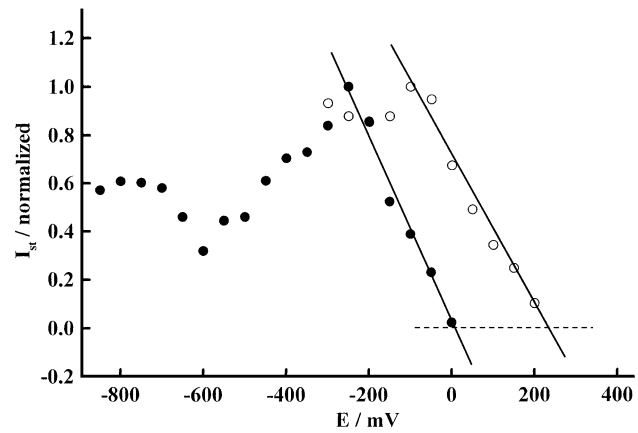

Fig. 4. Plot of the light-on stationary current I_{st} vs. E on DOPC-coated mercury under the conditions of Fig. 3 (solid circles) and on TET-coated mercury under the conditions of Fig. 5 (open circles). Both plots are normalized at the maximum negative light-on stationary current, set equal to unity.

appears from Fig. 4, which shows a plot of the stationary current I_{st} vs. E (solid circles). I_{st} is practically zero at +0.010 V. As the applied potential is shifted towards negative values, it increases linearly up to about −0.250 V, then decreases with a further negative shift up to about −0.600 V, where it starts increasing again. This behavior differs from that exhibited by the light-on photocurrent of PM fragments adsorbed on hexadecanethiol/DOPC mixed bilayers [11], which has no stationary component throughout the whole potential range investigated.

Adsorbing PM fragments on a TET-coated mercury electrode causes a decrease in its differential capacitance at −0.400 V from ~24 to ~5 μF cm^{-2}. This indicates that PM fragments have a strong tendency to be adsorbed on top of the TET monolayer. Fig. 5 shows the light-on and light-off currents obtained by shining PM fragments adsorbed on TET-coated mercury at different potentials. The thiol coating allows the recording of stable photo-

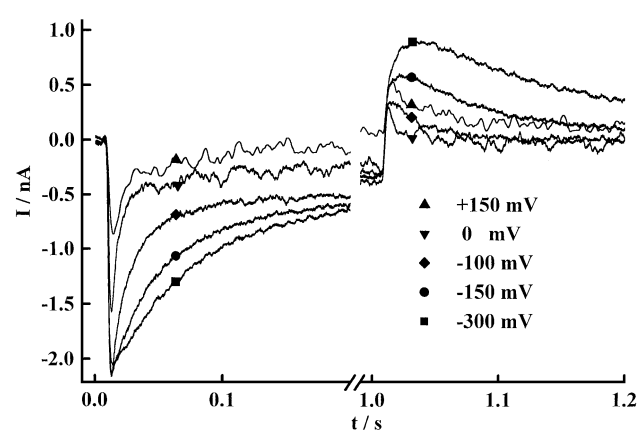

Fig. 5. Negative light-on currents and corresponding positive light-off currents obtained at different applied potentials from PM fragments adsorbed on a TET-coated mercury electrode immersed in a pH 6.75 buffered solution of 0.1 M KCl + 1 mM KH_2PO_4 + 1 mM K_2HPO_4.

currents up to potentials as positive as +0.300 V, in spite of a decrease in the signal-to-noise ratio. No hysteresis or change in the background current (i.e. the time-independent current recorded before illumination) is observed when carrying out repeated measurements on the same TET-coated drop. The photocurrents in Fig. 5 are qualitatively similar to those on DOPC-coated mercury in Fig. 3. However, the linear portion of the plot of the light-on stationary current I_{st} vs. E intersects the potential axis at ~ +0.230 V (open circles in Fig. 4).

Photocurrent measurements were also carried out on PM fragments adsorbed on a mercury-supported DOPC monolayer incorporating 1.5 mol% ubiquinone-10 (UQ). These measurements aimed at verifying the effect of the local decrease of pH produced by the proton pumping activity of bR in the cleft between the PM fragments and the lipid film upon the pH-dependent kinetics of UQ electroreduction to ubiquinol-10 (UQH_2). The formal potential of the UQ/UQH_2 redox couple in a DOPC monolayer in contact with the pH 8.6 buffered solution adopted in these measurements amounts to −0.220 V [28]. Before each measurement, the electrode was kept at −0.150 V to allow the complete oxidation to UQ of any UQH_2 molecules formed in previous measurements. The electrode was then kept at the potential of measurement until the background current was stabilized; this required usually from 3 to 5 min. Fig. 6 shows a number of light-on currents at different potentials obtained by illuminating this electrode. The light-on current attains its maximum value after about 50 ms of illumination. The presence of UQ starts affecting the light-on current only at potentials negative of about −0.350 V. The open circles in the inset of Fig. 6 are values of the excess charge due to the presence of UQ, which flows during the first 50 ms of illumination. This charge first increases rapidly and then tends to a saturation value.

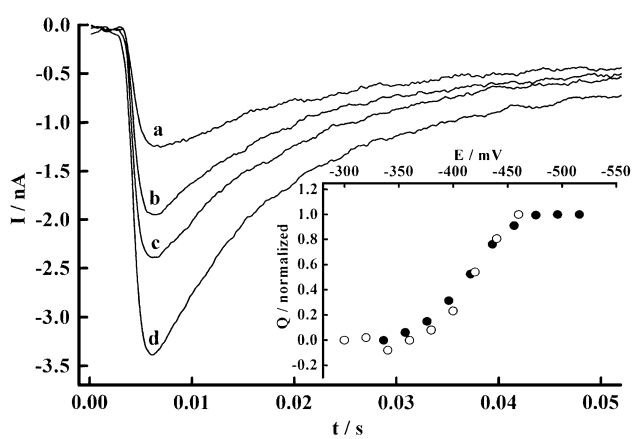

Fig. 6. Light-on currents obtained from PM fragments adsorbed on a mercury electrode coated with a DOPC monolayer incorporating 1.5 mol% UQ and immersed in a pH 8.6 buffered solution of 0.1 M KCl+5 mM H_3BO_3+1.2 mM NaOH. Applied potential: −0.360 (a), −0.380 (b), −0.400 (c) and −0.420 V (d). In the inset, the open circles are values of the integral, over the first 50 ms of illumination, of the photocurrent in the presence of UQ in excess to that in its absence at the same potential; the solid circles are values of the faradaic charge following a series of potential steps of the 50-ms length from E_i=−0.150 V to progressively more negative potentials E in the absence of PM fragments, under otherwise identical conditions. Both plots in the inset are normalized at their maximum value, set equal to unity.

4. Discussion

A significant difference between the bR light-on currents on a DOPC monolayer and on a mixed hexadecanethiol/DOPC bilayer [11], both supported by mercury, is represented by the presence of a nonzero stationary component in the former case, but not in the latter. In Ref. [11], to explain the presence of a finite light-off current on the mixed bilayer, it was necessary to assume the presence of a nonzero stationary component b_p of the pump current, i.e. a stationary proton flux across the photoexcited PM fragments. The fact that this continuous proton flux does not give rise to a stationary light-on current along the external circuit was explained by the following assumption: at some time before interrupting illumination, a steady state is attained in which the number of protons being pumped into the cleft between the PM fragments and the mixed bilayer is equal to those reaching the PM rim and moving towards the bulk solution in the same time. In practice, the latter proton movement completely bypasses the stationary pump current b_p. Consequently, no electron flow along the external circuit towards the mercury surface is required to keep the applied potential constant, and the light-on stationary current vanishes. This interpretation is supported by the experimental finding that protons move very rapidly along the surface of PM fragments suspended in an aqueous solution [29] and, more generally, along the polar heads of well-organized phospholipid monolayers [30–35].

The finite, potential-dependent stationary light-on current observed on a mercury-supported DOPC monolayer implies a continuous flow of electrons to the mercury surface along the external circuit, and therefore a continuous accumulation of protons between the PM fragments and the mercury surface, to keep the applied potential constant. In other words, the protons are no longer able to reach the PM rim rapidly, thus bypassing the stationary pump current. This behavior can be explained by considering that phospholipid monolayers on Hg are compact and impermeable to inorganic ions over a potential range from −0.200 to −0.75 V [14–16]. At more positive potentials, they become less organized, as denoted by an increase in differential capacity. This disorder may be increased by the adsorbed PM fragments, which may squeeze the monolayer or even penetrate into the hydrocarbon tail region. While protons are known to move very rapidly along a well-organized polar head region, this is no longer true with a disorganized lipid film, which may also allow an easy access of protons to the mercury surface. Naturally, the accumulation of protons cannot proceed indefinitely. The maximum stationary light-on current recorded for 2 min corresponds to the accumulation of a

charge density of 3.4 μC cm^{-2}. This is much less than the maximum charge density, about 40 μC cm^{-2}, due to specific adsorption on mercury of a typical inorganic ion such as chloride [36]. The constancy of the stationary (or, better, quasi-stationary) current during an illumination period of 2 min is therefore justified, even though the current is expected to decrease as illumination is prolonged to a sufficient extent.

The increase in the light-on stationary current with a negative shift in the applied potential from +0.010 to −0.250 V is explained by the translocation of protons across the membrane fragments being assisted by an electric field increasingly directed towards the electrode. At potentials negative of about −0.250 V, the DOPC molecules start to become more organized, with a resulting decrease in the differential capacitance C_m (see curve b in Fig. 2) and an increase in the resistance R_m of the lipid monolayer. This causes an increasing fraction of the potential difference across the interface to accumulate in the lipid film. As long as a negative shift in the applied potential E improves such an organization of the lipid monolayer, the potential difference across the PM may well become less negative, thus explaining the decrease in the stationary light-on current between −0.250 and −0.600 V. Such a decrease may also be favored by a more rapid movement of the pumped protons along the polar head region of the lipid monolayer. At potentials negative of −0.600 V, the lipid film tends again to become less compact and permeable to inorganic ions. Hence, the stationary current starts increasing again with a further negative shift in the applied potential, as shown in Fig. 4.

4.1. Fitting of bR photocurrents to an equivalent circuit

The behavior of the bR photocurrent on DOPC-coated mercury at potentials positive of −0.250 V (Fig. 3), with particular regard to the potential dependence of the stationary current I_{st}, can be interpreted on the basis of an equivalent circuit similar to that adopted to explain the behavior of bR photocurrents at a mercury-supported hexadecanethiol/DOPC bilayer [11]. However, in that circuit, bR was represented as a current source. Such a representation required the expression for the pump current I_p to be ascribed a priori. In particular, I_p was set equal to the sum of an exponentially decaying contribution $a_p\exp(-t/\tau)$ and of a stationary contribution b_p. This representation does not lend itself to the determination of the potential dependence of the stationary current I_{st} flowing along the external circuit. To achieve this goal, herein bR will be represented as a voltage source E_p, in series with a resistance R_2 and with a parallel arrangement of a resistance R_1 and a capacitance C_1 (Fig. 7). A gate function activates E_p at time $t=0$, when illumination is started, and deactivates it at $t=T$, when illumination is interrupted. The PM consists of the whole branch representing the bR, with in parallel, the resistance R_p and capacitance C_p of the PM. The branch representing the whole PM is in series with a parallel arrangement of the resistance R_m and capacitance C_m of the supporting phospholipid monolayer. The whole system is closed on the external applied potential E. The analysis of this equivalent circuit is summarized in Appendix A. In the absence of the R_mC_m mesh that simulates the DOPC monolayer, the branch representing bR generates a pump current I_p that consists of an exponentially decaying contribution and of a stationary one:

$$I_p = a_p\exp(-t/\tau_p)b_p = \frac{R_1E_p}{R_2(R_1+R_2)} \times \exp\left[-t\Big/\left(\frac{R_1R_2}{R_1+R_2}C_1\right)\right] + \frac{E_p}{R_1+R_2} \quad (1)$$

This equation shows that representing bR as a voltage source is equivalent to representing it as a current source. Eq. (1) allows the parameters R_1, R_2 and C_1, which depend exclusively upon the intrinsic properties of bR, to be estimated from the a_p, τ_p and b_p values of the current-source representation of bR adopted in Ref. [11], once the pump voltage E_p is known. The latter can be reasonably regarded as equal and opposite to the transmembrane potential, +250 mV, which must be applied across an oocyte membrane incorporating bR to annihilate the stationary pump current [23]. From the current-source parameters $a_p=-500$ nA

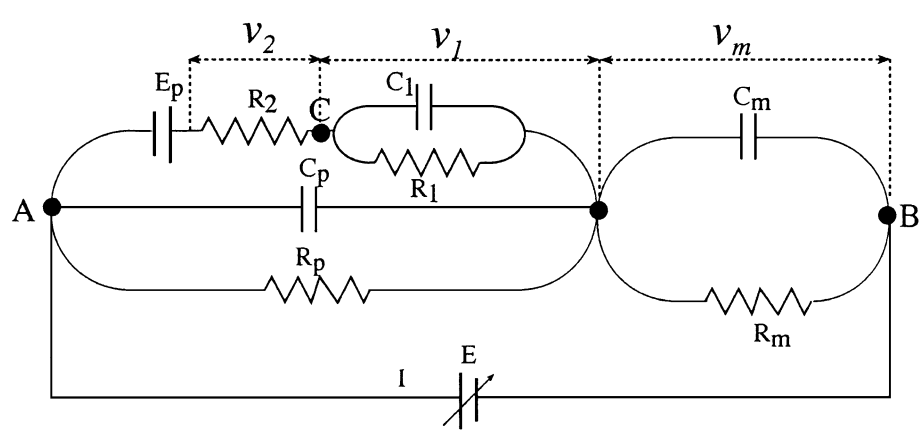

Fig. 7. Equivalent circuit adopted to interpret the photocurrents of PM fragments adsorbed on DOPC-coated mercury.

cm^{-2}, $\tau_p = 7.7$ ms and $b_p = -200$ nA cm^{-2}, as derived from the equivalent circuit employed to fit the photocurrents on a hexadecanethiol/DOPC bilayer at pH 6.4 [11], the voltage-source parameters $R_1 = 0.89$ MΩ cm^2, $R_2 = 0.36$ MΩ cm^2 and $C_1 = 30$ nF cm^{-2} are obtained.

Due to the presence of the supporting DOPC monolayer, the light-on current I flowing along the external circuit is obviously different from I_p. In particular, it has a stationary contribution $k[(R_1+R_2)E/R_p+E+E_p]$, where $k \equiv (\tau_1\tau_2\alpha\beta R_m)^{-1}$ is a constant that depends on all elements of the equivalent circuit. On the other hand, the stationary contribution to the light-off current is equal to $k[(R_1+R_2)E/R_p+E]$. Hence, the latter contribution is the background current I_{back}, namely the current that flows along the external circuit both in the absence and in the presence of illumination. The light-on stationary current, as measured with respect to the background current, is therefore equal to kE_p, and does not depend on the applied potential E, in disagreement with experiment. As a matter of fact, the equivalent circuit adopted herein blocks the voltage source as illumination is interrupted, but allows the current driven by the external applied potential E to continue flowing through the ion pump even in the dark. To exclude the latter event, which is expected to be hindered by an unfavorable conformation of bR in the dark, the stationary light-off current must be set equal to $k[(R_1+R_2)E/R_p]$, thus excluding the E-driven current, kE, that flows along the same bR channel as the current, kE_p, driven by the voltage source. Incidentally, the resulting background current, $I_{back} = k[(R_1+R_2)E/R_p]$, tends to $E/(R_m+R_p)$ for $R_m \to 0$ and $C_m \to \infty$, i.e. in the absence of the supporting lipid film, as expected. It should be noted that this change in background current involves an approximation in the analysis of the light-off current, since it is introduced into the expression for this current only a posteriori. On the basis of this approximation, the light-on stationary current measured with respect to the background current is now equal to $k(E+E_p)$. Therefore, it varies linearly with E, in accordance with experiment. This confirms the statement that no external applied potential can drive a current through bR in the dark.

To fit the equivalent circuit of Fig. 7 to the photocurrents on DOPC-coated mercury over the potential range from +0.010 to −0.250 V, the same PM resistance $R_p = 7.44$ kΩ cm^2 and capacity $C_p = 1.8$ μF cm^{-2} as used to fit the photocurrents on a hexadecanethol/DOPC bilayer [11] were adopted, together with the voltage-source parameters R_1, R_2 and C_1 extracted from the same independent fitting. Moreover, E_p was set equal to −250 mV. Therefore, only the resistance R_m and capacity C_m of the DOPC monolayer remained to be adjusted. The best fit to the experimental I vs. t curves, shown in Fig. 3 for three different applied potentials, was obtained for $R_m = 2.5 \times 10^4$ Ω cm^2 and $C_m = 1 \times 10^{-5}$ F cm^{-2}. This R_m value is in fairly good agreement with the resistance, 1.5×10^4 Ω cm^2, obtained from the linear dependence of the background current density upon the applied potential over the potential range from −0.250 to +0.050 V. As expected, the calculated light-off currents are appreciably different from the experimental ones, because of the approximation involved in their estimate. Conversely, the calculated light-on currents are in good agreement with the experimental ones, since they are not affected by this approximation. The low resistance and high capacitance of the DOPC film, as compared to those of a compact DOPC monolayer ($R_m \cong 5$ MΩ cm^2 and $C_m = 1.8$ μF cm^{-2}) confirm its disorganization over this positive potential range, most likely enhanced by the presence of PM fragments. In spite of the relatively low value of the time constant, $\tau_m = R_m C_m$, of the supporting lipid film, this is more than one order of magnitude greater that those, $\tau_1 = R_1 C_1$ and $\tau_3 = R_2 C_1$, of the proton pump. Consequently, the exponential decay of the photocurrent is mainly controlled by bR. Since the values of the circuit elements R_1, R_2 and C_1, representing bR as a voltage source on a supporting lipid monolayer, were extracted from the circuit elements representing bR as a current source on a supporting thiol/lipid mixed bilayer, this confirms the consistency between the results obtained with these two different supporting materials by using two different equivalent circuits.

4.2. Extrathermodynamic absolute potential difference across the mercury/water interphase

The light-on stationary current of PM fragments adsorbed on a mercury-supported DOPC monolayer vanishes at an applied potential E of about +0.010 V, while that of an oocyte membrane incorporating bR vanishes for a transmembrane potential of +250 mV [23]. It is therefore reasonable to assume that at $E = +0.010$ V the potential difference across the PM fragments is approximately equal to +250 mV. To verify this point, extrathermodynamic assumptions are required. In fact, only the transmembrane potential is thermodynamically significant and experimentally accessible without recourse to modelistic assumptions, being the potential difference between two phases of identical composition (i.e. the aqueous phases that bath the two sides of the biomembrane). This is no longer true for the potential difference across a PM fragment adsorbed on a solid support. The first step consists in estimating the extrathermodynamic absolute potential difference ϕ across the whole mercury/solution interphase. If mercury is coated with a self-assembled lipid monolayer having a neutral polar head, such as DOPC, ϕ can be approximately expressed by the equation:

$$\phi = \chi_e + \chi_m + 4\pi\left(\frac{\beta}{\varepsilon_\beta} + \frac{\gamma}{\varepsilon_\gamma}\right)\sigma_M + \phi_d \qquad (2)$$

Here σ_M is the charge density on the metal, β and γ are the thickness of the hydrocarbon tail and of the polar head region, ε_β and ε_γ are the corresponding distortional dielectric

constants, χ_e is the surface dipole potential due to the electron spillover, χ_m is the surface dipole potential due to the oriented polar heads, and ϕ_d is the potential difference across the diffuse layer (Fig. 8) [20]. At physiological ion concentrations, ϕ_d can be disregarded as a good approximation. Moreover, the orientation of the polar heads of the lipid film is hardly affected by changes in σ_M. The differential capacitance C of the electrode can, therefore, be written:

$$\frac{d\phi}{d\sigma_M} \equiv \frac{1}{C} = -4\pi x_{im} + 4\pi\left(\frac{\beta}{\varepsilon_\beta} + \frac{\gamma}{\varepsilon_\gamma}\right)$$
$$\text{with}: \frac{d\chi_e}{d\sigma_M} = -4\pi x_{im}; \frac{d\chi_m}{d\sigma_M} \cong 0 \quad (3)$$

Here, the contribution $d\chi_e/d\sigma_M$ to the reciprocal of the interfacial capacitance from the inhomogeneous electron gas is expressed on the basis of the jellium model by $-4\pi x_{im}$ [37], where x_{im} is the "position of the effective image plane", i.e. the distance from the surface atoms of the metal at which the idealized, perfectly conducting metal-surface plane should be placed to account for electron spillover. x_{im} is always positive, ranging from 0.5 to 1 Å, and hence makes a positive contribution to C. In the presence of a lipid monolayer, whose hydrocarbon chain has a length β of the order of 20 Å and a dielectric constant ε_β of about 2, this contribution is negligibly small; this is even more true for its possible changes with a change in σ_M. Within the limits in which both the differential capacitance C and the dipole potential χ_m due to the orientation of the polar heads at a given potential E can be regarded as independent of potential over the potential range from E to the potential of zero charge (pzc), from Eqs. (2) and (3), it follows that the absolute potential difference ϕ at the applied potential E is given by:

$$\phi - \chi_e = \sigma_M/C + \chi_m \quad (4)$$

In deriving Eq. (4), ϕ_d and $4\pi x_{im}$ were disregarded on the basis of the previous considerations. As long as the metal is coated with a self-assembled film, the dipole potential χ_e due to the electron spillover can be regarded as constant *for the given metal* in view of its small rate of change, $-4\pi x_{im}$, with a change in the charge density σ_M on the metal. However, in passing from the bare metal in contact with an aqueous solution to the same metal coated with a self-assembled film, a certain change in χ_e cannot be excluded. For the present purposes, the dipole potential χ_e for a given metal will be regarded as approximately constant with varying the solution side of the interphase. Within the limits of this approximation, the expression of $\phi - \chi_e$ in Eq. (4) can be regarded as an extrathermodynamic absolute potential difference across the whole interphase between the given metal and the bulk aqueous phase: it will be denoted by ψ. Both σ_M and C in Eq. (4) are experimentally accessible and thermodynamically significant. If χ_m can be determined independently on the basis of extrathermodynamic arguments, then the extrathermodynamic absolute value of $\psi(E)$ at the given applied potential E is obtained. Once $\psi(E)$ is known, it holds independent of the particular nature of the interphase interposed between the metal and the bulk aqueous phase. Moreover, the absolute value of the potential $\psi(E')$ at a different applied potential E' differs from that, $\psi(E)$, at E by the difference, $(E' - E)$, between the two applied potentials relative to the same reference electrode.

An accurate estimate of the charge density σ_M at a mercury electrode coated with a DOPC monolayer and immersed in aqueous 0.1 M tetramethylammonium chloride at -0.450 V/SCE yields a value of -0.75 μC cm^{-2} [38]. Application of Eq. (4) to this electrode yields:

$$\psi(-450\ \text{mV/SCE}) = \frac{\sigma_M}{C} + \chi_m = \frac{-0.75\ \mu C\ \text{cm}^{-2}}{1.8\ \mu F\ \text{cm}^{-2}} + (200 \pm 50)\ \text{mV} \cong -(200 \pm 50)\ \text{mV} \quad (5)$$

where the differential capacity of a DOPC monolayer was set equal to 1.8 μF cm^{-2} [14–16]. The dipole potential χ_m

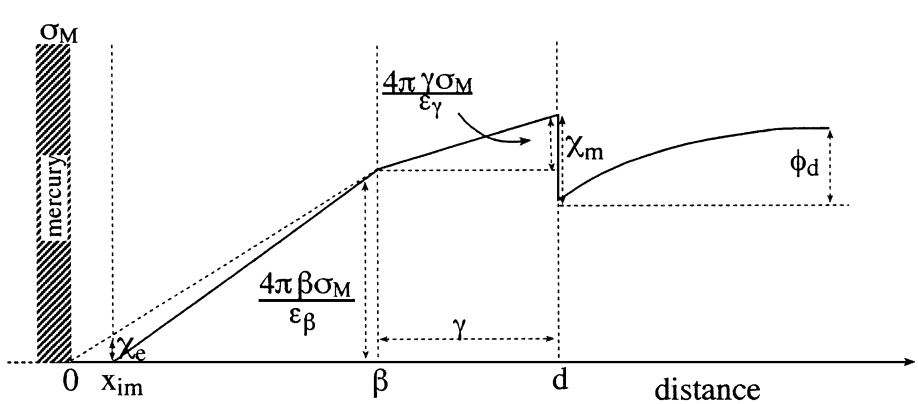

Fig. 8. Schematic picture of the model of a neutral phospholipid monolayer deposited on mercury. The solid curve schematically represents the profile of the average potential against the distance from the mercury surface. For clarity, the diffuse-layer thickness has been compressed and x_{im} has been enlarged with respect to the monolayer thickness.

due to the oriented polar heads of the DOPC monolayer has been estimated by different procedures both on BLMs [39–42] and on a mercury electrode [43], and the literature values range from +150 to +250 mV, positive towards the hydrocarbon tails. An average value of +200 mV was therefore adopted in Eq. (5). The absolute potential difference between mercury and the aqueous phase can, therefore, be obtained by increasing the applied potential vs. the SCE by about 250 mV.

From the above arguments, it follows that the absolute potential difference ψ across the whole mercury/(aqueous solution) interphase at +0.010 V, where the bR stationary light-on current vanishes, amounts to about +260 mV. This value is in fairly good agreement with the corresponding transmembrane potential, +250 mV, across an oocyte plasma membrane incorporating bR [23]. From such a comparison, it follows that, at potentials positive of −0.250 V, the PM fragments experience by far the majority of the whole potential difference across the interphase. Since the surface dipole potential of the polar heads of a well-organized DOPC monolayer amounts to about +200 mV, this confirms the conclusion that at potentials positive of −0.250 V, the film is strongly disorganized, particularly in the presence of adsorbed PM fragments. Quite probably, the lipid molecules are strongly tilted and, possibly, almost flat on the mercury surface, thus making a small contribution to the surface dipole potential. It is also possible that at these positive potentials, the PM squeezes out the lipid film coming in direct contact with the electrode.

On TET-coated mercury, the light-on stationary current vanishes at about +0.230 V, as shown in Fig. 4. At this potential, bare mercury undergoes bulk oxidation to Hg_2Cl_2 in a chloride solution. To understand this behavior, the limiting value of the charge that flows at +0.250 V on TET-coated mercury was measured by carrying out a potential step from −0.500 to +0.250 V. After about 3 min, the resulting charge attains a maximum limiting value of about +3 mC cm^{-2}, which corresponds to the formation of about 40 Hg_2Cl_2 monolayers. Therefore, at these far positive potentials, the PM fragments are practically adsorbed on a more or less disordered TET monolayer on top of an Hg/Hg_2Cl_2/(0.1 M KCl) electrode. The potential of this calomel electrode is about 90 mV more positive than that of a saturated calomel reference electrode. Hence, the potential difference across the system (TET monolayer+PM fragment) at +0.230 V amounts to about +0.320 V. In view of the complex and probably disordered structure of the interphase at these positive potentials, this potential difference can be regarded as not too far from the transmembrane potential, +250 mV, across an oocyte plasma membrane incorporating bR [23]. However, a small contribution from the surface dipole potential of the TET monolayer cannot be excluded. It is interesting to observe that PM fragments are directly adsorbed on mercury at potentials positive of +0.100 V, even in the absence of a TET or DOPC coating. The resulting electrode, once photoexcited, yields scarcely reproducible photocurrents.

4.3. Effect of bR photocurrent on ubiquinone-10 electroreduction

The incorporation of 1.5 mol% UQ in the DOPC monolayer causes a rapid increase in the peak current and in the charge under the light-on current transient at potentials negative of −0.350 V (Fig. 6). This behavior is explained by considering that the UQ molecules incorporated in the portion of DOPC monolayer covered by PM fragments are prevented from being electroreduced to UQH_2 at potentials negative of the formal potential of the UQ/UQH_2 couple during the 3–5 min required to stabilize the background current. This is due to the difficulty encountered by the protons involved in the rate-determining step $UQ^{-\cdot}+H^{+}\rightarrow UQH^{\cdot}$ [44] to penetrate into the lipid film covered by the PM fragments. This difficulty was proven by adsorbing PM fragments on a pure UQ monolayer self-assembled on mercury. Upon PM adsorption, the voltammetric peak III_c for UQ electroreduction was notably depressed and shifted in the negative direction, as shown in Fig. 9. Moreover, peaks I and II, due to phase transitions of the UQ film [45], were completely suppressed. The solid circles in the inset of Fig. 6 are values of the chrono-

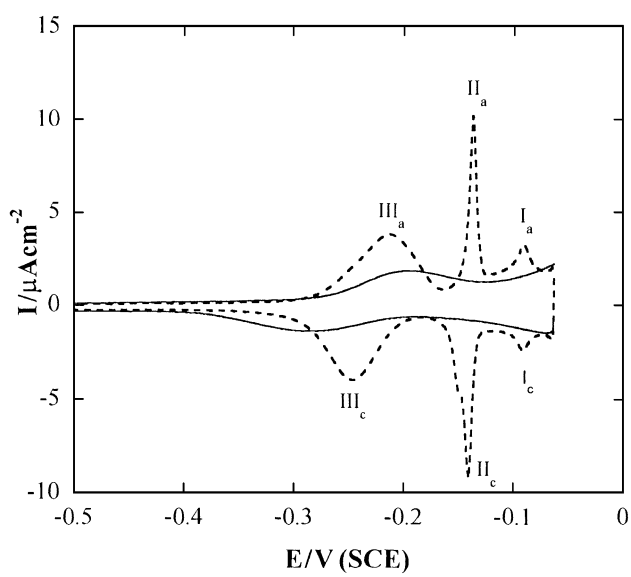

Fig. 9. Cyclic voltammogram of a pure UQ monolayer supported by a mercury electrode immersed in a pH 8.6 buffered solution of 0.1 M KCl with (solid curve) and without (dashed curve) PM fragments adsorbed on top of the monolayer. The monolayer was obtained by immersing an HMDE in the electrolyte solution on whose surface 0.2 μg cm^{-2} of UQ had been previously spread. In the dashed curve, peaks I and II are due to two-dimensional phase transitions of the UQ monolayer [45], peak III_c is due to UQ electroreduction, and peak III_a to UQH electrooxidation.

coulometric faradaic charge for the electroreduction of 1.5 mol% UQ incorporated in a mercury-supported DOPC monolayer in contact with a pH 8.6 buffered solution, as a function of the applied potential E. This curve was obtained by recording the charge, $Q(E,t=50$ ms), following a series of steps from a fixed initial potential $E_i=-0.150$ V to progressively more negative potentials E; the charge was recorded after 50 ms from the instant of each potential step. The curve of $Q(E,t=50$ ms) vs. E closely parallels that of the excess photocharge due to the presence of 1.5 mol% UQ vs. E. This indicates that the pumping activity of the photoexcited PM fragments provides the underlying UQ molecules with a proton activity in the cleft between the PM and the lipid film that is comparable with that in the bulk solution, at least during the first 50 ms of illumination.

Acknowledgements

The authors are grateful to Prof. E. Bamberg (Max-Planck-Institut für Biophysik, Frankfurt/Main) for providing them with the PM and to Prof. S. Evans (Centre for Self-Organising Molecular Systems, University of Leeds, UK) for providing them with the triethyleneoxythiol. Bracco and Prof. C. de Häen are gratefully acknowledged for a PhD fellowship to A.D. during the tenure of which the present results were obtained. The financial support of the Ministero dell'Universita' e della Ricerca Scientifica e Tecnologica of Italy and of the Ente Cassa di Risparmio di Firenze is gratefully acknowledged.

Appendix A

Node analysis applied to nodes A, B and C in the equivalent circuit of Fig. 7 yields the three differential equations:

$$I=\frac{v_2}{R_2}+C_p\frac{d(E-v_m)}{dt}+\frac{E-v_m}{R_p}$$

$$\text{(a)};\ I=C_m\frac{dv_m}{dt}+\frac{v_m}{R_m}\ \text{(b)};\quad \frac{v_2}{R_2}=C_1\frac{dv_1}{dt}+\frac{v_1}{R_1}\ \text{(c)} \tag{A1}$$

$$\text{with}:\quad E=-E_pG(t,T)+v_1+v_2+v_m \tag{A2}$$

Here $G(t,T)$ is a gate function. Eqs. (A1) and (A2) are combined to obtain a differential equation for v_m, which is Laplace transformed making use of the relationship $L\{dG(t,T)/dt\}=[1-\exp(-sT)]/s$. Inverse Laplace transformation and substitution of the resulting expression for $v_m(t)$ into Eq. (A1-b) yields the following expression for the current:

$$\begin{aligned}I=&\frac{b/\alpha-a+v_m(0-)\alpha}{(\alpha-\beta)R_m}(1-\alpha\tau_m)e^{-\alpha t}\\&-\frac{b/\beta-a+v_m(0-)\beta}{(\alpha-\beta)R_m}(1-\beta\tau_m)e^{-\beta t}+\frac{b}{\alpha\beta R_m}\\&-\frac{E_p}{\tau_1\tau_2\alpha\beta R_m}S(t-T)-\frac{E_p}{\tau_2(\alpha-\beta)R_m}\\&\times\left[\left(\frac{1}{\tau_1\alpha}-1\right)(1-\alpha\tau_m)e^{-\alpha(t-T)}-\left(\frac{1}{\tau_1\beta}-1\right)\right.\\&\left.\times(1-\beta\tau_m)e^{-\beta(t-T)}\right]S(t-T)\end{aligned}$$

where $S(t-T)$ is a step function and:

$$R\equiv R_pR_m/(R_p+R_m);\ C\equiv C_p+C_m;\ \tau\equiv RC;$$
$$\tau_1\equiv R_1C_1;\ \tau_2\equiv R_2C;\ \tau_3\equiv R_2C_1;\ \tau_m\equiv R_mC_m$$

$$p\equiv\tau^{-1}+\tau_1^{-1}+\tau_2^{-1}+\tau_3^{-1};$$
$$q\equiv(\tau\tau_1)^{-1}+(\tau\tau_3)^{-1}+(\tau_1\tau_2)^{-1}$$

$$\alpha\equiv\left(p-\sqrt{p^2-4q}\right)/2;\ \beta\equiv\left(p+\sqrt{p^2-4q}\right)/2$$

$$a\equiv\frac{E}{R_pC}+\frac{v_m(0-)}{\tau_3}\left(\frac{R_2}{R_1}+1\right)+\frac{E+E_p-v_1(0-)}{\tau_2};$$
$$b\equiv\frac{1}{\tau_1\tau_2}\left(\frac{R_1+R_2}{R_p}E+E+E_p\right)$$

It follows that the background current, i.e. the current flowing in the dark, is given by:

$$I_{back}=\frac{1}{\tau_1\tau_2\alpha\beta R_m}\left(\frac{R_1+R_2}{R_p}E+E\right)\equiv k\left(\frac{R_1+R_2}{R_p}E+E\right)$$

In the absence of the supporting lipid film, i.e. for $R_m\to 0$ and $C_m\to\infty$, the expression of the current simplifies as follows:

$$\begin{aligned}I=&\frac{R_1E_p}{R_2(R_1+R_2)}\exp\left[-t\Big/\left(\frac{R_1R_2}{R_1+R_2}C_1\right)\right]+\frac{E}{R_p}\\&+\frac{E+E_p}{R_1+R_2}-\frac{E_p}{R_1+R_2}S(t-T)-\frac{R_1E_p}{R_2(R_1+R_2)}\\&\times\exp\left[-(t-T)\Big/\left(\frac{R_1R_2}{R_1+R_2}C_1\right)\right]S(t-T)\end{aligned}$$

The pump current I_p, which flows in the time interval from 0 to T, is obtained from the above equation by setting $E=0$; it is given by Eq. (1) in the text.

References

[1] J. Heberle, Proton transfer reactions across bacteriorhodopsin and along the membrane, Biochim. Biophys. Acta 1458 (2000) 135–147.

[2] L.S. Brown, Reconciling crystallography and mutagenesis: a synthetic approach to the creation of a comprehensive model for proton pumping by bacteriorhodopsin, Biochim. Biophys. Acta 1460 (2000) 49–59.
[3] J.K. Lanyi, Crystallographic studies of the conformational changes that drive directional transmembrane ion movement in bacteriorhodopsin, Biochim. Biophys. Acta 1459 (2000) 339–345.
[4] S.P. Balashov, Protonation reactions and their coupling in bacteriorhodopsin, Biochim. Biophys. Acta 1460 (2000) 75–94.
[5] S. Subramaniam, R. Henderson, Crystallographic analysis of protein conformational changes in the bacteriorhodopsin photocycle, Biochim. Biophys. Acta 1460 (2000) 157–165.
[6] N.A. Dencher, H.J. Sass, G. Büldt, Water and bacteriorhodopsin: structure, dynamics, and function, Biochim. Biophys. Acta 1460 (2000) 192–203.
[7] H. Kandori, Role of internal water molecules in bacteriorhodopsin, Biochim. Biophys. Acta 1460 (2000) 177–191.
[8] H. Luecke, Atomic resolution structures of bacteriorhodopsin photocycle intermediates: the role of discrete water molecules in the function of this light-driven ion pump, Biochim. Biophys. Acta 1460 (2000) 133–156.
[9] A.D. Kaulen, Electrogenic processes and protein conformational changes accompanying the bacteriorhodopsin photocycle, Biochim. Biophys. Acta 1460 (2000) 204–219.
[10] K. Seifert, K. Fendler, E. Bamberg, Charge transport by ion translocating membrane proteins on solid supported membranes, Biophys. J. 64 (1993) 384–391.
[11] A. Dolfi, F. Tadini Buoninsegni, M.R. Moncelli, R. Guidelli, Photocurrents generated by bacteriorhodopsin adsorbed on thiol/lipid bilayers supported by mercury, Langmuir, in press.
[12] A. Dolfi, F. Tadini Buoninsegni, G. Aloisi, M.R. Moncelli, Bacteriorhodopsin-containing membrane fragments adsorbed on mercury-supported biomimetic membranes, Electrochem. Commun. 1 (1999) 131–134.
[13] R. Guidelli, G. Aloisi, L. Becucci, A. Dolfi, M.R. Moncelli, F. Tadini Buoninsegni, Interfacial bioelectrochemistry: assessment and trends, J. Electroanal. Chem. 504 (2001) 1–28.
[14] A. Nelson, A. Benton, Phopholipid monolayers at the mercury/water interface, J. Electroanal. Chem. 202 (1986) 253–270.
[15] M.R. Moncelli, L. Becucci, R. Guidelli, The intrinsic pK_a values for phosphatidylcholine, phosphatidylethanolamine and phosphatidylserine in monolayers deposited on mercury electrodes, Biophys. J. 66 (1994) 1969–1980.
[16] M.R. Moncelli, L. Becucci, R. Herrero, R. Guidelli, Adsorption of tetraphenylphosphonium and tetraphenylborate in self-assembled phosphatidylcholine and phosphatidylserine monolayers deposited on mercury electrodes, J. Phys. Chem. 99 (1995) 9940–9951.
[17] D. Oesterhelt, W. Stoeckenius, Isolation of the cell membrane of *Halobacterium halobium* and its fractionation into red and purple membrane, Methods Enzymol. 31 (1974) 667–678.
[18] L. Becucci, M.R. Moncelli, R. Guidelli, Surface charge density measurements on mercury electrodes covered by phospholipid monolayers, J. Electroanal. Chem. 413 (1996) 187–193.
[19] M.R. Moncelli, L. Becucci, A novel model of the hanging mercury drop electrode, J. Electroanal. Chem. 433 (1997) 91–96.
[20] M.R. Moncelli, L. Becucci, F. Tadini Buoninsegni, R. Guidelli, Surface dipole potential at the interface between water and self-assembled monolayers of phosphatidylserine and phosphatidic acid, Biophys. J. 74 (1998) 2388–2397.
[21] B. Robertson, E.P. Lukashev, Rapid pH change due to bacteriorhodopsin measured with a tin-oxide electrode, Biophys. J. 68 (1995) 1507–1517.
[22] A. Fahr, P. Laüger, E. Bamberg, Photocurrent kinetics of purple-membrane sheets bound to planar bilayer membranes, J. Membr. Biol. 60 (1981) 51–62.
[23] G. Nagel, B. Kelety, B. Möckel, G. Büldt, E. Bamberg, Voltage dependence of proton pumping by bacteriorhodopsin is regulated by the voltage-sensitive ratio of M1 to M2, Biophys. J. 74 (1998) 403–412.
[24] J. Tittor, U. Schweiger, D. Oesterhelt, E. Bamberg, Inversion of proton translocation in bacteriorhodopsin mutants D85N, D85T, and D85,96N, Biophys. J. 67 (1994) 1682–1690.
[25] H.J. Butt, K. Fendler, E. Bamberg, J. Tittor, D. Oesterhelt, Aspartic acids 96 and 85 play a central role in the function of bacteriorhodopsin as a proton pump, EMBO J. 8 (1989) 1657–1663.
[26] R. Borlinghaus, H.J. Apell, P. Läuger, Fast charge translocations associated with partial reactions of the Na,K-pump: I. Current and voltage transients after photochemical release of ATP, J. Membr. Biol. 97 (1987) 161–178.
[27] K. Fendler, S. Jaruschewski, A. Hobbs, W. Albers, J.P. Froehlich, Presteady-state charge translocation in NaK-ATPase from eel electric organ, J. Gen. Physiol. 102 (1993) 631–666.
[28] M.R. Moncelli, R. Herrero, L. Becucci, R. Guidelli, Kinetics of electron and proton transfer to ubiquinone-10 and from ubiquinol-10 in a self-assembled phosphatidylcholine monolayer, Biochim. Biophys. Acta 1364 (1998) 373–384.
[29] J. Heberle, J. Riesle, G. Thiedemann, D. Oesterhelt, N.A. Dencher, Proton migration along the membrane surface and retarded surface to bulk transfer, Nature 370 (1994) 379–382.
[30] D.B. Kell, On the functional proton current pathway of electron transport phosphorylation. An electrodic view, Biochim. Biophys. Acta 549 (1979) 55–99.
[31] M. Prats, J.-F. Tocanne, J. Teissié, Lateral proton conduction at a lipid/water interface, Eur. J. Biochem. 149 (1985) 663–668.
[32] J. Teissié, M. Prats, P. Soucaille, J.-F. Tocanne, Evidence for conduction of protons along the interface between water and a polar lipid monolayer, Proc. Natl. Acad. Sci. U. S. A. 82 (1985) 3217–3221.
[33] M. Prats, J. Teissié, J.-F. Tocanne, Lateral proton conduction at lipid–water interfaces and its application for the chemiosmotic-coupling hypothesis, Nature 322 (1986) 756–758.
[34] H. Morgan, D.M. Taylor, O.N. Oliveira Jr., Two-dimensional proton conduction at a membrane surface: influence of molecular packing and hydrogen bonding, Chem. Phys. Lett. 150 (1988) 311–314.
[35] Y.N. Antonenko, O.N. Kovbasnjuk, L.S. Yaguzhinsky, Evidence in favor of the existence of a kinetic barrier for proton transfer from a surface of bilayer phospholipid membrane to bulk water, Biochim. Biophys. Acta 1150 (1993) 45–50.
[36] D.C. Grahame, R. Parsons, Components of charge and potential in the inner region of the electrical double layer: aqueous potassium chloride solutions in contact with mercury at 25 °C, J. Am. Chem. Soc. 83 (1961) 1291–1296.
[37] W. Schmickler, in: J. Lipkowski, P.N. Ross (Eds.), Structure of Electrified Interfaces, VCH, New York, 1993, pp. 201–238.
[38] F. Tadini Buoninsegni, L. Becucci, M.R. Moncelli, R. Guidelli, Total and free charge densities on mercury coated with self-assembled phosphatidylcholine and octadecanethiol monolayers and octadecanethiol/phosphatidylcholine bilayers, J. Electroanal. Chem. 500 (2001) 395–407.
[39] R.J. Clarke, Effect of lipid structure on the dipole potential of phosphatidylcholine bilayers, Biochim. Biophys. Acta 1327 (1997) 269–278.
[40] A.D. Pickar, R. Benz, Transport of oppositely charged lipophilic probe ions in lipid bilayer membranes having various structures, J. Membr. Biol. 44 (1978) 353–376.
[41] K. Gawrisch, D. Ruston, J. Zimmerberg, V.A. Parsegian, R.P. Rand, N. Fuller, Membrane dipole potentials, hydration forces, and the ordering of water at membrane surfaces, Biophys. J. 61 (1992) 1213–1223.
[42] R.F. Flewelling, W.L. Hubbell, The membrane dipole potential in a total membrane potential model. Application to hydrophobic ion interactions with membranes, Biophys. J. 49 (1986) 541–552.
[43] L. Becucci, M.R. Moncelli, R. Herrero, R. Guidelli, Dipole potentials

of self-assembled monolayers of dioleoylphosphatidylcholine, dioleoylphosphatidylserine and dioleoylphosphatidic acid on mercury, Langmuir 16 (2000) 7694–7700.

[44] M.R. Moncelli, L. Becucci, A. Nelson, R. Guidelli, Electrochemical modeling of electron and proton transfer to ubiquinone-10 in a self-assembled phospholipid monolayer, Biophys. J. 70 (1996) 2716–2726.

[45] G.J. Gordillo, D.J. Schiffrin, Redox properties of ubiquinone (UQ_{10}) adsorbed on a mercury electrode, J. Chem. Soc., Faraday Trans. 90 (1994) 1913–1922.